

Different conformational families of pyrimidine·purine·pyrimidine triple helices depending on backbone composition

Hogyu Han and Peter B.Dervan*

The Beckman Institute, California Institute of Technology, Pasadena, CA 91125, USA

Received January 18, 1994; Revised and Accepted May 12, 1994

ABSTRACT

Different helical conformations of DNA (D), RNA (R), and DNA·RNA (DR) hybrid double and triple helices have been detected using affinity cleavage analysis. Synthetic methods were developed to attach EDTA·Fe to a single nucleotide on RNA as well as DNA oligonucleotides. Cleavage patterns generated by a localized diffusible oxidant in the major groove on the pyrimidine strand of four purine·pyrimidine double helices consisting of all DNA, all RNA, and the corresponding hybrids reveal that the relative cleavage intensity shifts to the 5' end of the purine strand increasingly in the order: DD < DR < RD < RR. These results are consistent with models derived from structural studies. In six pyrimidine·purine·pyrimidine triple helices, the altered cleavage patterns of the Watson–Crick pyrimidine strands reveal at least two conformational families: (i) D + DD, R + DD, D + DR, and R + DR and (ii) R + RD and R + RR.

INTRODUCTION

Three studies of the energetics of triple helix formation by a combination of RNA and DNA strands show different triple helical stabilities depending on backbone composition (1–3). A pyrimidine RNA strand binds double helical DNA, RNA, and DNA·RNA hybrids, whereas a pyrimidine DNA strand binds duplexes only when the purine strand of the duplex is DNA (1–3). It would appear that there could be several conformational families of triple helices related to the sugar identities of the three strands. The presence or absence of the 2'-hydroxyl on the sugar that distinguishes RNA from DNA likely determines the conformational preference for A- or B-form duplexes with C-3' endo and C-2' endo sugar conformations, respectively. RNA duplexes prefer to adopt an A-form helical structure, whereas DNA duplexes can adopt B- or A-form (4–6). In DNA·RNA hybrid duplexes, the RNA strand retains an A-like C3'-endo conformation, whereas the DNA strand is not 3'-endo (7–10). With regard to triple helices, all RNA (U)_n + (rA)_n(U)_n, all DNA (T)_n + (dA)_n(T)_n, and hybrids (U)_n + (dA)_n(U)_n are shown to be all A-form by X-ray fiber diffraction studies (11–13). However,

recent structural studies of all DNA triple helices indicate that the triple helix has a B-form conformation with C2'-endo sugar pucker (14–17).

A DNA binding molecule equipped with EDTA·Fe cleaves DNA by oxidation of the deoxyribose backbone via a nonspecific diffusible oxidant, presumably hydroxyl radical, allowing nucleotide positions proximal to the cleaving moiety in the DNA structure to be mapped to nucleotide resolution by high-resolution gel electrophoresis (18–22). EDTA·Fe located in the major groove of right-handed DNA generates an asymmetric cleavage pattern with maximal cleavage loci shifted to the 5' side on the opposite strands (20–22) (Figure 1). The question arises whether the asymmetric shift is sensitive to differences in helical conformations. If so, then affinity cleaving analysis might detect differences in all DNA, all RNA, and hybrid triple helices. Since there is a body of literature on the differences in DNA and RNA double helices, we first tested DNA·DNA, RNA·RNA, and hybrid double helices as a control. Based on these results, we then analyzed the triple helices.

Affinity cleaving using oligoribonucleotide-EDTA (RNA-EDTA) requires a synthetic method for the introduction of EDTA·Fe at unique positions of RNA. We describe here synthesis of RNA-EDTA oligonucleotides and their use to study the conformations of double and triple helical complexes. RNA-EDTA and DNA-EDTA with uridine-EDTA (*U) and thymidine-EDTA (*T), respectively, located at common positions were prepared by the incorporation of phosphoramidites of the functionalizable uridine and 2'-deoxyuridine derivatives into oligonucleotides followed by a post-automated synthesis modification. First, we examined conformations of DNA, RNA, and DNA·RNA hybrid double helices. The results reveal that for the sequences studied here, the cleavage pattern on the purine strand generated by *U and *T located at the same position on the pyrimidine strand in purine·pyrimidine double helical DD, DR, RD, and RR gradually shifts from 3' to 5', respectively. These findings agree qualitatively with structural data from x-ray analysis, confirming the usefulness of affinity cleaving to investigate differences in helical geometries. The cleavage pattern observed for the pyrimidine strand of the Watson–Crick duplex in triple helices suggests two triple helical conformational

*To whom correspondence should be addressed

families: (i) D+DD, R+DD, D+DR, and R+DR and (ii) R+RD and R+RR. These results indicate that helical geometries of triple helices are different depending on backbone composition.

MATERIALS AND METHODS

General

^1H NMR spectra were recorded at 300 MHz on a GE 300 NMR in $\text{DMSO}-d_6$. Chemical shifts are reported in ppm downfield from tetramethylsilane. High-resolution mass spectra (HRMS) were recorded using fast atom bombardment techniques at the Mass Spectrometry Laboratory at the University of California, Riverside. Preparative HPLC was performed on a Hewlett Packard 1050 Series preparative HPLC using a Vydac C18 reverse phase column (1.0×25 cm, $5 \mu\text{m}$, TP silica). Analytical HPLC was performed on a Hewlett Packard 1090 Series II analytical HPLC using a Vydac C18 reverse phase column (0.46×25 cm, 5 mm, HS silica). Flash chromatography was carried out using silica gel 60 (230–400 mesh, Merck). Thin-layer chromatography (TLC) was performed on silica gel 60 F₂₅₄ precoated plates (Merck). All chemicals for the synthesis were purchased from Aldrich unless otherwise specified. Acetonitrile, pyridine, dichloromethane, tetrahydrofuran (THF), and *N,N*-dimethylformamide (DMF) were purchased as anhydrous solvents from Aldrich. Phosphoramidites were purchased from Applied Biosystems (dA, dG, dC, and T) and from BioGenex Laboratories (San Ramon, CA) (rA, rG, rC, and U).

Nucleoside 2

Nucleoside 1 was prepared as described (23,24). To a solution of 1 (2.7 g, 6.87 mmol) in CH_3OH (100 mL) was added 10% palladium on carbon (300 mg) and the mixture was shaken under H_2 (50 psi) for 10 h. The reaction mixture was filtered through Celite and the filtrate was evaporated to dryness to give 2.6 g

(97%) of a white solid. TLC (4% $\text{H}_2\text{O}/\text{CH}_3\text{CN}$) $R_f=0.39$; ^1H NMR δ 11.34 (s, 1H), 9.44 (t, $J=5.8\text{Hz}$, 1H), 7.75 (s, 1H), 5.77 (d, $J=5.3\text{Hz}$, 1H), 5.37 (d, $J=5.7\text{Hz}$, 1H, 2'OH), 5.09 (m, 2H, 5'OH + 3'OH), 4.04 (m, 1H), 3.97 (m, 1H), 3.82 (m, 1H),

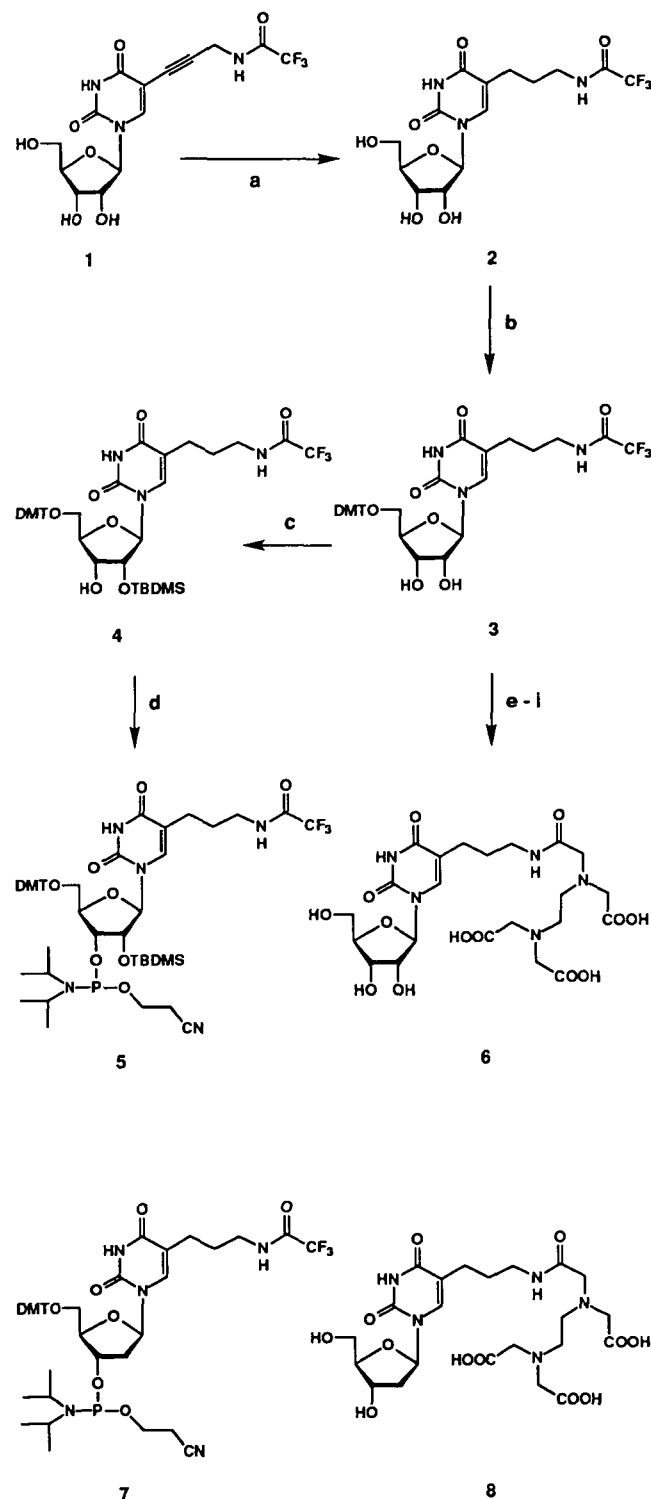


Figure 2. (Upper) Scheme for the synthesis of phosphoramidite 5 and *U 6. Reaction conditions: (a) Pd/C, MeOH; (b) DMT·Cl, pyridine; (c) TBDMS·Cl, AgNO₃, pyridine; (d) $[(\text{CH}_3)_2\text{CH}]_2\text{NP}(\text{Cl})\text{OCH}_2\text{CH}_2\text{CN}$, DIEA, THF; (e) NH_3 /ethanol; (f) activated EDTA(Et)₃; (g) TFA; (h) 0.1 N NaOH; (i) acetic acid. (Lower) Phosphoramidite 7 and *T 8.

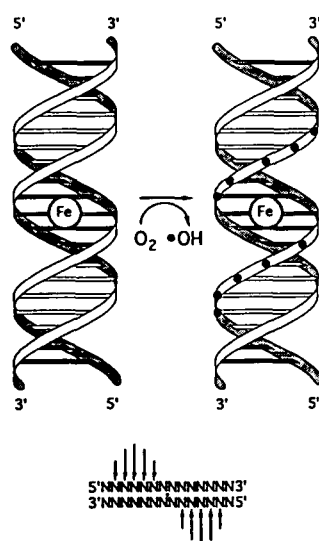


Figure 1. Cleavage patterns produced by a diffusible oxidant generated by EDTA·Fe localized in the major groove of right-handed DNA. The edges of the bases are shown as open bars for the minor groove and crosshatched for the major groove, respectively. The filled circles show points of cleavage along the phosphodiester deoxyribose backbone.

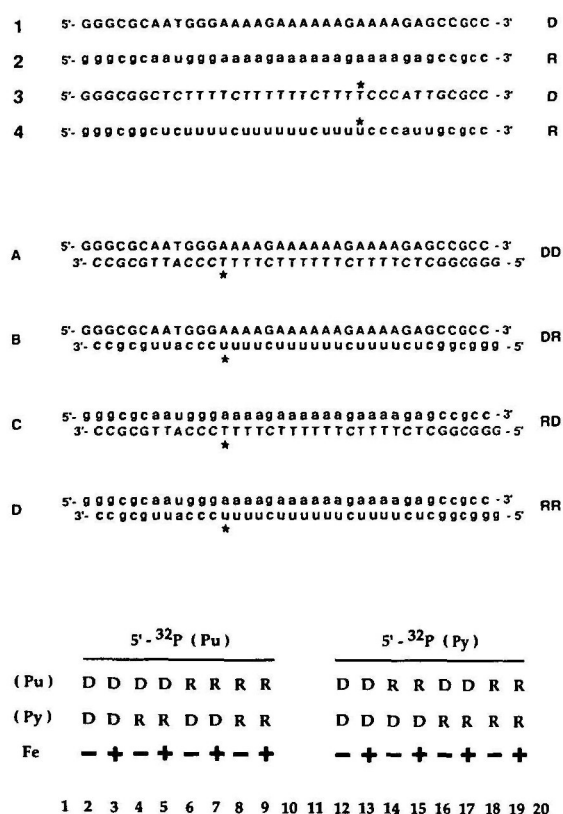


Figure 5. (Upper) Sequences of DNA-EDTA (3), RNA-EDTA (4), and 35-bp duplexes DD (1 + 3), DR (1 + 4), RD (2 + 3), and RR (2 + 4). The uppercase letters indicate DNA and the lowercase letters, RNA. (Lower) Autoradiogram of a 20% denaturing polyacrylamide gel showing affinity cleavage reactions. (Lane 2, 4, 6, 8, 12, 14, 16, 18) Control showing intact 5' labeled duplex standard obtained after treatment according to the cleavage reactions in the absence of Fe. (Lane 3, 5, 7, 9, 13, 15, 17, 19) Affinity cleavage products produced in the presence of Fe. (Lane 1) A-specific chemical sequencing of (5'-³²P PuD)(PyD) (34). (Lane 10, 20) A+U enzymatic sequencing (Phy M) of (5'-³²P PuR) and (5'-³²P PyR), respectively (35). (Lane 11) T-specific chemical sequencing (KMnO₄) of (5'-³²P PyD) (36). Watson and Crick strands are indicated by (Pu) and (Py), where D indicates DNA and R, RNA.

THF (2 mL) for 2 h (19). The mixture was concentrated and redissolved in 1% trifluoroacetic acid (TFA) in CH₂Cl₂ (10 mL). After stirring for 1 h at 25°C, the mixture was concentrated and then allowed to react with 0.1 N NaOH (10 mL). After 10 h at 55°C, the mixture was neutralized with acetic acid, concentrated, and desalted (Sephadex LH-20 column, Pharmacia). The crude mixture was purified by preparative HPLC. The products were eluted with solvent A (0.1% TFA in H₂O) with a gradient of 3–5% solvent B (0.08% TFA in CH₃CN) over 20 min at a flow rate of 2 mL/min and detection was UV absorption at 260 nm. The fractions containing products were combined and evaporated to dryness to afford 0.045 g (56%) of a white solid. ¹H NMR (DMSO-*d*₆/1% D₂O) δ 11.30 (s, 1H), 8.13 (t, *J*=5.6 Hz, 1H), 7.76 (s, 1H), 5.77 (d, *J*=5.4 Hz, 1H), 4.06 (m, 1H), 3.98 (m, 1H), 3.82 (m, 1H), 3.59 (m, 2H), 3.45 (s, 4H),

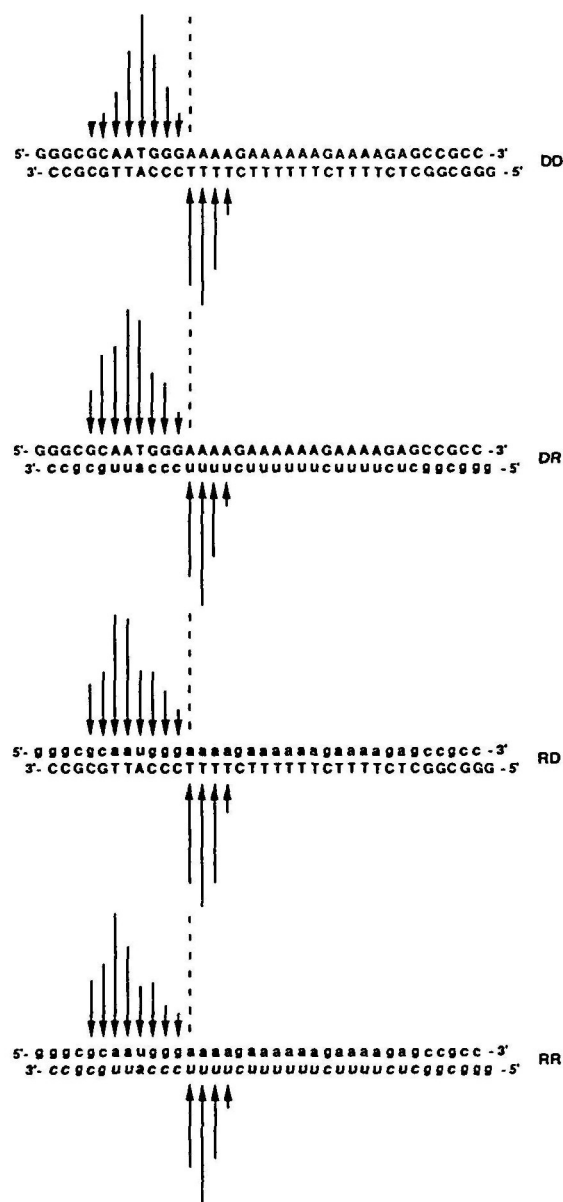


Figure 6. Histograms of the cleavage data derived from the autoradiogram in Figure 5.

3.38 (s,2H), 3.23 (s,2H), 3.09 (m,2H), 2.75 (bs,4H), 2.17 (m,2H), 1.57 (m,2H); HRMS for $C_{22}H_{34}N_5O_{13}$ $[MH]^+$, calcd 576.2153, found 576.2128.

Phosphoramidite 7

Synthesized according to the procedure as described (25).

Thymidine-EDTA 8 (*T)

Synthesized according to the procedure for *U 6. Yield=52%; 1H NMR (DMSO- d_6 /1% D_2O) δ 11.29 (s,1H), 8.13 (t, J =5.6Hz,1H), 7.70 (s,1H), 6.17 (t, J =6.8Hz,1H), 4.24 (m,1H), 3.76 (m,1H), 3.57 (m,2H), 3.47 (s,4H), 3.42 (s,2H), 3.27 (s,2H), 3.09 (m,2H), 2.77 (bs,4H), 2.21–2.06 (m,4H), 1.56 (m,2H); HRMS for $C_{22}H_{34}N_5O_{12}$ $[MH]^+$, calcd 560.2203, found 560.2193.

EDTA-triester 10

To a solution of ethylenediaminetetraacetic dianhydride (EDTA-dianhydride, 10.8 g, 42.2 mmol) in DMF (150 mL) were added 2-(trimethylsilyl)ethanol (16.4 g, 138.6 mmol) and 4-dimethylaminopyridine (DMAP, 1.5 g, 12.2 mmol). After stirring at 45°C for 12 h, 1-(3-dimethylaminopropyl)-3-ethylcarbodiimide hydrochloride (EDCI, 8.85 g, 46.1 mmol) was added. The solution was stirred for 8 h at 25°C, concentrated, and purified by flash chromatography using 7% CH_3OH/CH_2Cl_2 to yield 5.1 g (20%) of a yellow oil. TLC (10% CH_3OH/CH_2Cl_2) R_f =0.40; 1H NMR δ 4.09 (t, J =8.4Hz,6H), 3.50 (s,6H), 3.32 (s,2H), 2.70 (bs,4H), 0.92 (t, J =8.4Hz,6H), 0.02 (s,27H); HRMS for $C_{25}H_{53}N_2O_8Si_3$ $[MH]^+$, calcd 593.3111, found 593.3082.

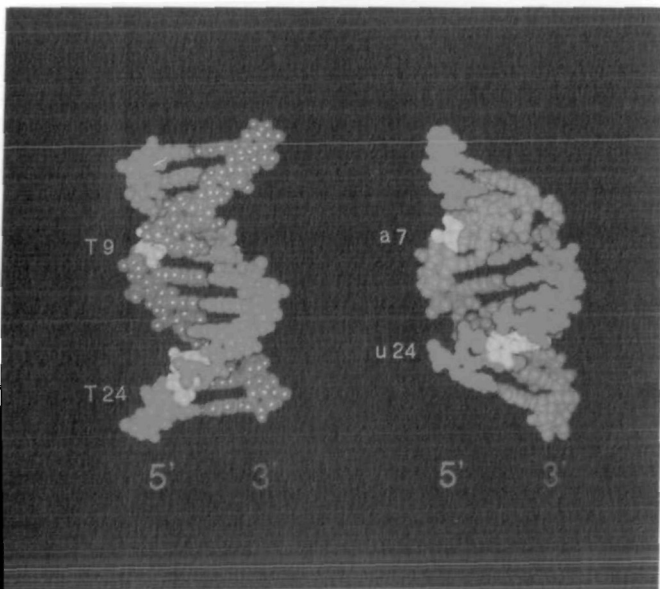


Figure 7. Schematic representation of B-form DNA (left) and A-form RNA (right) of the sequences (GCAA(T/U)GGGAAA) obtained by using the Biopolymer module of Insight II (version 2.2.0) from Biosym Technologies. The purine strand is shown in red and the pyrimidine strand in blue. The sugars of the maximal cleavage sites on the purine and pyrimidine strand are shown in yellow and the thymine and uridine bases on the pyrimidine strand where *T and *U are placed are shown in white.

RNA-EDTA and DNA-EDTA synthesis

Oligoribonucleotides and oligodeoxyribonucleotides were synthesized on an Applied Biosystems Model 394 DNA/RNA synthesizer using 2-cyanoethyl phosphoramidite chemistry. Phosphoramidites 5 and 7 (0.15 M solutions in CH_3CN) were incorporated into RNA and DNA, respectively. RNA (1 μ mol) containing nucleoside 5 was deprotected by treatment with NH_3 saturated methanol (4 mL) at 25°C for 24 h and lyophilized. The crude RNA oligonucleotides (0.2 μ mol) in THF (50 μ L) were treated with 0.3 M activated EDTA-triester 11 in DMF (100 μ L). After stirring at 25°C for 10 min, the reaction was stopped by addition of H_2O (150 μ L) and dried. Removal of the silyl protecting groups was carried out in tetrabutylammonium fluoride (TBAF, 300 μ L of 1 M solutions in THF) at 25°C for 24 h. The resulting solution was dried, desalted with a NAP-5 column (Pharmacia) and purified on a 20% polyacrylamide/7 M urea gel. DNA (1 μ mol) containing nucleoside 7 was deprotected with NH_4OH (4 mL) at 55°C and lyophilized. The crude DNA oligonucleotides (0.2 μ mol) in 200 mM borate (50 μ L, pH 8.9) were treated with 0.3 M activated EDTA-triethylester 12 in DMF (100 μ L). After stirring at 25°C for 10 min, the reaction was stopped by addition of H_2O (150 μ L) and dried. Removal of the ethyl protecting groups was carried out in 0.1 N NaOH (1 mL) at 55°C for 24 h and neutralized with acetic acid. The resulting mixture was applied to a Sephadex G10–120 column and eluted with H_2O . The crude oligonucleotides were lyophilized and then purified on a 20% polyacrylamide/7 M urea gel.

An alternative procedure for the modification of RNA and DNA by either EDTA dianhydride or EDTA monoanhydride was performed as follows (26,27). The completely deprotected RNA (5 nmol) or DNA (5 nmol) in 0.2 M $NaHCO_3$ (50 μ L, pH 8.17) was treated with either EDTA dianhydride (25 μ L of 1% w/v DMF solution) or EDTA monoanhydride (5 mg) for 2 h at 25°C. The reactions were quenched by addition of 100 mM Tris–HCl buffer pH 7.2 (25 μ L) and H_2O (150 μ L), followed by ethanol precipitation. After the crude oligonucleotide-EDTA with a reduced electrophoretic mobility was purified on 20% polyacrylamide/7 M urea gels, UV-absorbing bands were excised, crushed, and eluted (0.3 M NaOAc, pH 5.2, 37°C, 24 h). The resulting solutions were filtered (0.45- μ m Centrex filter, Schleicher and Schuell) and desalted (NAP-5 column).

HPLC analysis of RNA-EDTA and DNA-EDTA

The purified oligonucleotide-EDTA (5 nmol) was digested simultaneously with snake venom phosphodiesterase (5 μ L, 2 μ g/ μ L, Sigma) and calf intestine alkaline phosphatase (5 μ L, 1 unit/ μ L, Pharmacia) in 50 mM Tris–HCl (pH 8.1), 100 mM $MgCl_2$ at 37°C for 2 h (50 μ L final volume). A filtered aliquot (20 μ L) was analyzed by analytical HPLC. The products were eluted with solvent A (250 mM Triethylamine–acetate pH 6.0, 1 mM EDTA) with a gradient of 15–20% solvent B (CH_3OH) over 10 min at a flow rate of 1 mL/min and monitored by UV absorption at 260 nm. Comparison and co-injection with a standard solution containing rC, U, *U, dC, T, and *T established the composition of the oligonucleotides. The extinction coefficient (260 nm) used for *U and *T was 8,800 $cm^{-1} \cdot M^{-1}$.

Affinity cleavage reactions of double helical DNA, RNA, and DNA–RNA hybrids

DNA, DNA-EDTA, and RNA-EDTA oligonucleotides, 36 nt in length, were prepared by chemical synthesis as described

above. RNA oligonucleotides, 36 nt in length, were prepared by enzymatic synthesis using T7 RNA polymerase (Pharmacia) and dephosphorylated with calf intestine alkaline phosphatase before labeling (28). DNA and RNA were 5'-end labeled using γ - ^{32}P -ATP (≥ 3000 Ci/mmol, Amersham) and T4 polynucleotide kinase (New England Biolabs) (29). The 5'- ^{32}P -end-labeled duplex was prepared by hybridizing labeled strands

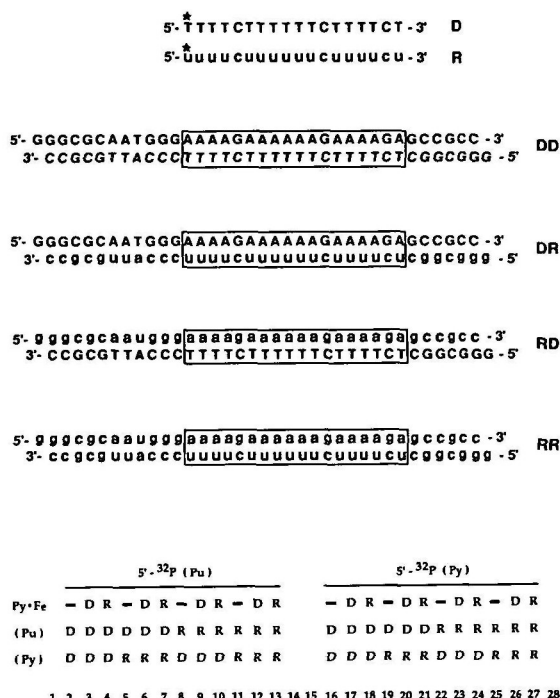


Figure 8. (Upper) Sequences of DNA-EDTA (D), RNA-EDTA (R), and 35-bp duplexes DD, DR, RD, and RR. The uppercase letters indicate DNA and the lowercase letters, RNA. The box indicates the 18-bp purine target sequence within the 35-bp duplex bound by D or R. (Lower) Autoradiogram of a 20% denaturing polyacrylamide gel showing affinity cleavage reactions. (Lane 2, 5, 8, 11, 16, 19, 22, 25) Control showing intact 5' labeled 35-bp duplex standard obtained after treatment according to the cleavage reactions in the absence of oligonucleotide-EDTA·Fe. (Lane 3, 4, 6, 7, 9, 10, 12, 13, 17, 18, 20, 21, 23, 24, 26, 27) Affinity cleavage products produced in the presence of oligonucleotide-EDTA·Fe. (Lane 1) A-specific chemical sequencing of (5'- ^{32}P PuD)(PyD). (Lane 14, 28) A+U enzymatic sequencing of (5'- ^{32}P PuR) and (5'- ^{32}P PyR), respectively. (Lane 15) T-specific chemical sequencing of (5'- ^{32}P PyD). Hoogsteen strands are indicated by Py-Fe and Watson and Crick strands are indicated by (Pu) and (Py), where D indicates DNA and R, RNA.

with their unlabeled complementary strands in 200 mM NaCl, 1 mM EDTA at 37 °C and purified with a 15% nondenaturing polyacrylamide gel. The 5'-end-labeled duplex was extracted with 200 mM NaCl and filtered through a 0.45- μm filter, followed by ethanol precipitation. The cleavage reactions were carried out by adding $\text{Fe}(\text{NH}_4)_2(\text{SO}_4)_2 \cdot 6\text{H}_2\text{O}$ (10 μM) to the ^{32}P -labeled 35-bp (base pairs) duplex DD, DR, RD, or RR ($\sim 20,000$ cpm) in 50 mM Tris·acetate, pH 7.0, 100 mM NaCl and then incubating at 25°C for 2h. Cleavage reactions were initiated by addition of dithiothreitol (4 mM) and allowed to proceed for 4 h at 25°C. The reactions were stopped by ethanol precipitation and the cleavage products were analyzed by gel electrophoresis.

Affinity cleavage reactions of triple helical DNA, RNA, and DNA·RNA hybrids

Labeled 35-bp double helical DNA and RNA oligonucleotides were prepared as described above. The cleavage reactions were carried out by combining a mixture of oligonucleotide-EDTA D or R (2 μM) and $\text{Fe}(\text{NH}_4)_2(\text{SO}_4)_2 \cdot 6\text{H}_2\text{O}$ (2.2 μM) with the ^{32}P -labeled 35-bp duplex DD, DR, RD, or RR ($\sim 20,000$ cpm) in association buffer (50 mM Tris·acetate, pH 7.0, 100 mM NaCl, 1 mM spermine, and 200 μM bp calf thymus DNA (Pharmacia)) and then incubating at 25°C for 2h. Cleavage reactions were initiated by addition of dithiothreitol (4 mM) and allowed to proceed for 4 h at 25°C. The reactions were stopped by ethanol precipitation and the cleavage products were analyzed by gel electrophoresis.

Affinity cleavage analysis

Histograms of the cleavage data were derived by densitometry of the autoradiogram. The cleavage intensity at a particular nucleotide was normalized using the cleavage intensity at the nucleotide cleaved the most efficiently in each strand. Arrow heights indicate the extent of cleavage at the indicated base.

RESULTS AND DISCUSSION

Synthesis and purification of oligoribonucleotide-EDTA

For the synthesis of oligoribonucleotides equipped with EDTA, a method compatible with RNA synthesis and deprotection conditions was developed, which involves the modification of RNA oligonucleotides containing a primary amine linked to the 5' position of uridine by EDTA derivatives such as EDTA protected with the 2-(trimethylsilyl)ethyl ester, EDTA dianhydride, and EDTA monoanhydride. The primary amino group linked to the 5' position of uridine-alkylamine **5** is revealed for modification by treatment with ammonia/methanol. Activated EDTA esters can be employed to modify RNA oligonucleotides before TBAF treatment and 2-(trimethylsilyl)ethyl esters can be deprotected by TBAF treatment. Alternatively, fully deprotected oligoribonucleotides with nucleoside **5** can be modified by either EDTA dianhydride or EDTA monoanhydride.

A scheme for the synthesis of phosphoramidites **5** is shown in Figure 2. Hydrogenation of **1** afforded **2**. The 5'-hydroxyl group of **2** was protected as the DMT ether to give **3**. Subsequent reaction of **3** with TBDMS·Cl afforded **4** (**30**). Activation of **4** with 2-cyanoethyl *N,N*-diisopropylchlorophosphoramidite afforded phosphoramidites **5**.

The EDTA-triester **10** was prepared from EDTA dianhydride in a one-pot reaction in 20% yield (Figure 3). The EDTA-triethylester was synthesized by copper-mediated monohydrolysis of the tetraethyl ester of EDTA (**19**).

Oligonucleotides were synthesized by automated methods using 2-cyanoethyl phosphoramidite chemistry (31,32). The phosphoramidites **5** and **7** were incorporated into RNA and DNA with 90–95% coupling efficiency. Deprotection of oligoribonucleotides with anhydrous saturated methanolic ammonia at 25°C affected the concomitant cleavage of oligonucleotides from the support and removal of the amino and phosphate protecting groups, leaving the 2'-O-silyl ethers intact (Figure 4). The functionalizable oligoribonucleotides with 2'-TBDMS groups were modified using the activated EDTA-triester **11**. Silyl groups on the 2' position and EDTA were removed by treatment with TBAF. The crude RNA-EDTA was desalted with Sephadex-G-25. Base labile protecting groups of oligodeoxyribonucleotides

were removed by treatment with 30% NH_4OH . Oligodeoxynucleotides with the same alkylamino-linker were allowed to react with the activated EDTA-triester **12**, followed by deprotection with 0.1 N NaOH. RNA-EDTA and DNA-EDTA were purified on a 20% denaturing polyacrylamide gel. A 40 nt RNA modified with EDTA can be resolved from an unmodified one on a 20% gel of 0.8 mm thickness. Enzymatic digestion of oligonucleotide-EDTA with snake venom phosphodiesterase and calf intestine alkaline phosphatase was carried out to confirm the integrity of *U, **6** and *T, **8** by HPLC.

Analysis of the double helix by affinity cleaving

The structure of each of four 35-bp duplexes, DD, DR, RD, and RR, was characterized by affinity cleaving (Figure 5). For this, *U and *T modified with EDTA at the 5' position were incorporated into the same position of the 36-nt pyrimidine strand in the Watson-Crick duplex. 10 mM concentration of $\text{Fe}(\text{NH}_4)_2(\text{SO}_4)_2 \cdot 6\text{H}_2\text{O}$ was mixed with 5'-end-labeled duplex containing *U and *T in buffer (50 mM Tris·acetate, pH 7.0, 100 mM NaCl, 25°C) and dithiothreitol was added to initiate cleavage. Histograms revealing the positions and extent of cleavage are shown in Figure 6. The cleavage patterns are nearly identical in the pyrimidine strands, whereas the position of maximal cleavage observed on opposite purine strands is shifted to the 5' direction in the order: DD, DR, RD, and RR. These results are consistent with structural data from x-ray studies. The cleavage efficiency at a nucleotide position is related to its distance in space from the *T/*U. This distance is determined by two parameters: the axial rise per nucleotide residue (h) and the twist angle (t) of the helix. Both h and t change when going from B-form to A-form duplexes and the predicted changes are consistent with the observed changes seen in the cleavage pattern. For example, maximal cleavage on the purine strand occurs four and

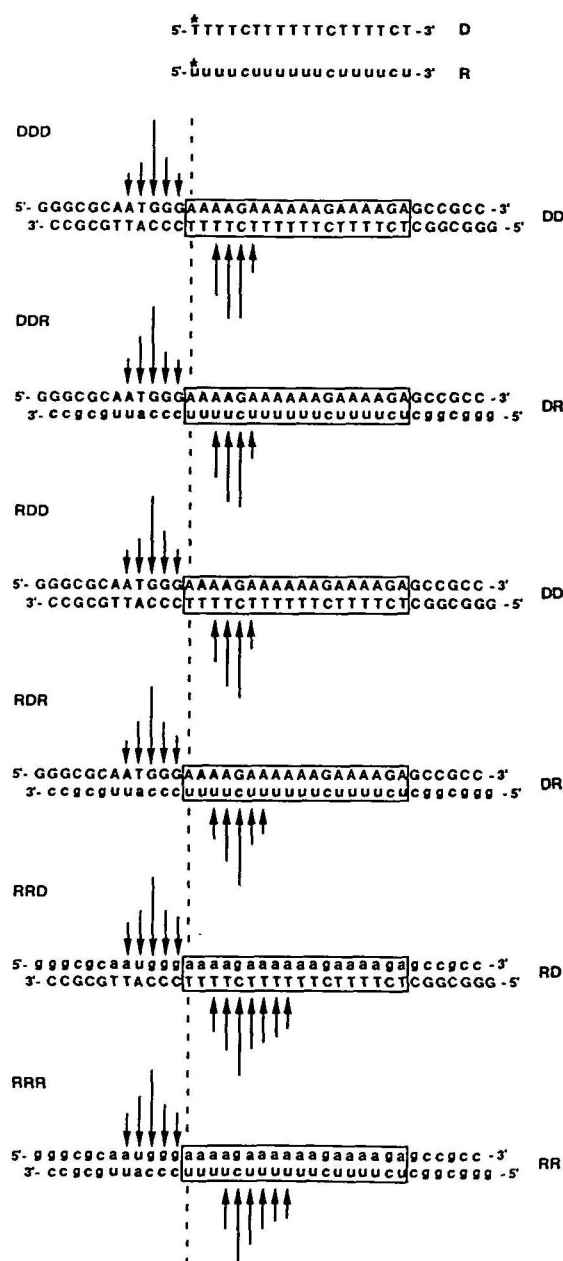


Figure 9. Histograms of the cleavage data derived from the autoradiogram in Figure 8.

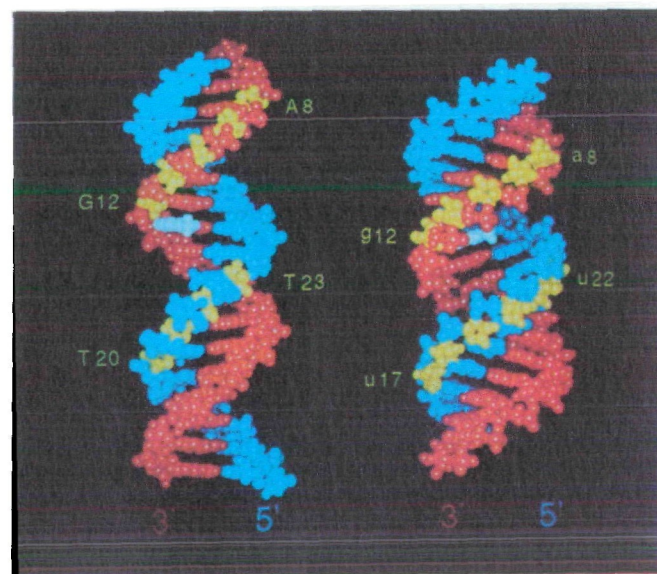


Figure 10. Models of the structures of base triplets built on B-form DNA (left) and A-form RNA (right) of the sequences (CAA(T/U)GGGAAAAGAAAAAA) obtained as described in Figure 7. The purine strand is shown in red and the pyrimidine strand in blue. The sugars of the cleavage sites on the Watson-Crick purine and pyrimidine strands are shown in yellow. The thymidine and uridine bases on the third strand where *T and *U are placed to form *T·AT and *U·AU base triplets are shown in white.

six nucleotides to the 5' side of *T and *U in double helical DD and RR, respectively. Upon going from B-form to A-form duplexes, the more distant nucleotide position in A-form RNA is brought closer in space to EDTA·Fe relative to the same position in B-form DNA due to the change in h and t ($h=3.38$ Å, $t=36^\circ$ for B-form DNA (3); $h=2.81$ Å, $t=32.7^\circ$ for A-form RNA (5)) (Figure 7). This leads to the different cleavage patterns seen between B-form DNA and A-form RNA duplexes. These findings confirm that affinity cleaving analysis is a sensitive method for detecting differences in helical conformations. The cleavage patterns of the two hybrids fall in between double helical DD and RR. Similar results were obtained from a gel mobility study of purine·pyrimidine double helices (DNA>hybrids>RNA) (2). These results indicate that it is unlikely that all hybrid helices adopt an A-form double helical structure ($h=3.03$ – 3.46 Å, $t=32.7^\circ$ or 36° for poly(rA)·poly(T) (7); $h=3.06$ Å, $t=32.7^\circ$ for poly(dA)·poly(U) (8)).

Analysis of the triple helix by affinity cleaving

Oligonucleotides RNA- and DNA-EDTA·Fe (D and R) (18 nt in length) were allowed to bind to 18 bp purine·pyrimidine tracts within each of four 35-bp duplexes, DD, DR, RD, and RR (Figure 8). For this, 5'-end-labeled duplex and 2 mM concentration of an oligonucleotide-EDTA·Fe D or R were mixed in association buffer. Affinity cleavage reactions were performed on six triple helical complexes comprised of combinations of DNA and RNA. Oligonucleotide D forms a stable triple helix only with DD and DR whereas oligonucleotide R forms a stable complex with all DD, DR, RD, and RR (Figure 9). For all cases, oligonucleotides D and R bind parallel to the purine strand of the Watson–Crick duplexes. An asymmetric cleavage pattern with maximal cleavage shifted to the 5' side of U* or T* on the opposite strands was observed, indicating that oligonucleotides D and R are located in the major groove of the Watson–Crick duplexes. Comparison of histograms reveals that the similar cleavage pattern is observed for all purine strands of the Watson–Crick duplex in the six triple helices, whereas the cleavage pattern on the pyrimidine strands of the Watson–Crick duplex appears different between two triple helical groups: (i) D+DD, R+DD, D+DR, and R+DR and (ii) R+RD and R+RR. R+RD and R+RR give additional cleavage at sites closer to the 5' end of the pyrimidine strand. In Figure 10, the cleavage patterns for D+DD and R+RR triple helical complexes are mapped to B-form DNA and A-form RNA double helices, respectively. The cleavage sites cover four and six nucleotides, with the most distal cleavage five and eight nucleotides to the 5' side of *T and *U on the pyrimidine strand in D+DD and R+RR triple helices, respectively. All these sites are proximal to EDTA·Fe located on the third strand in the major groove of the Watson–Crick B-form DNA and A-form RNA. The proximity of these cleavage sites to EDTA·Fe in space correlates with the high and low twist angle and axial rise per residue in B-form DNA and A-form RNA, respectively. Based on these results, it would appear that the Watson–Crick DNA duplex in the D+DD triple helix adopts a different helical conformation compared to the RNA duplex in the R+RR triple helix. The DNA or RNA identity of the purine strand of the Watson–Crick duplex seems to be a determinant of the triple helix conformation. Elucidation of parameters such as helical twist, axial rise per residue, sugar pucker, X-displacement, and base-pair inclination that distinguish one triple helical family from

the other must now await mutidimensional NMR and x-ray experiments (33).

ACKNOWLEDGEMENT

We are grateful to the National Institutes of Health for grant support.

REFERENCES

1. Roberts, R.W. and Crothers, D.M. (1992) *Science*, 258, 1463–1466.
2. Han, H. and Dervan, P.B. (1993) *Proc. Natl. Acad. Sci. U.S.A.*, 90, 3806–3810.
3. Escudé, C., Francois, J.-C., Sun, J.-S., Ott, G., Sprinzl, M., Garestier, T. and Helene, C. (1993) *Nucleic Acids Res.*, 21, 5547–5553.
4. Saenger, W. (1984) *Principles of Nucleic Acids Structure*, Springer-Verlag, New York.
5. Dock-Bregeon, A.C., Chevrier, B., Podjarny, A., Johnson, J., de Bear, J.S., Gough, G.R., Gilham, P.T. and Moras, D. (1989) *J. Mol. Biol.*, 209, 459–474.
6. Chou, S.-H., Flynn, P. and Reid, B. (1989) *Biochemistry*, 28, 2422–2435.
7. Zimmerman, S.B. and Pfeiffer, B.H. (1981) *Proc. Natl. Acad. Sci. U.S.A.*, 78, 78–82.
8. Arnott, S., Chandrasekaran, R., Millane, R.P. and Park, H.-S. (1986) *J. Mol. Biol.*, 188, 631–640.
9. Chou, S.-H., Flynn, P. and Reid, B. (1989) *Biochemistry*, 28, 2435–2443.
10. Salazar, M., Fedoroff, O.Y., Miller, J.M., Ribeiro, S. and Reid, B.R. (1993) *Biochemistry*, 32, 4207–4215.
11. Arnott, S. and Bond, P.J. (1973) *Nature New Biol.*, 244, 99–101.
12. Arnott, S. and Selsing, E. (1974) *J. Mol. Biol.*, 88, 509–521.
13. Arnott, S., Bond, P.J., Selsing, E. and Smith, P.J.C. (1976) *Nucleic Acids Res.*, 3, 2459–2470.
14. Macaya, R.F., Schultze, P. and Feigon, J. (1992) *J. Am. Chem. Soc.*, 114, 781–783.
15. Macaya, R.F., Wang, E., Schultze, P., Sklenar, V. and Feigon, J. (1992) *J. Mol. Biol.*, 225, 755–773.
16. Howard, F.B., Todd Miles, H., Liu, K., Frazier, J., Raghunathan, G. and Sasisekharan, V. (1992) *Biochemistry*, 31, 10671–10677.
17. Ouali, M., Letellier, R., Adnet, F., Liquier, J., Sun, J.-S., Lavery, R. and Taillandier, E. (1993) *Biochemistry*, 32, 2098–2103.
18. Hertzberg, R.P. and Dervan, P.B. (1984) *Biochemistry*, 23, 3934–3945.
19. Taylor, J.S., Schultz, P.G. and Dervan, P.B. (1984) *Tetrahedron*, 40, 457–465.
20. Sluka, J.P., Griffin, J.H., Mack, D.P. and Dervan, P.B. (1990) *J. Am. Chem. Soc.*, 112, 6369–6374.
21. Dreyer, G.B. and Dervan, P.B. (1985) *Proc. Natl. Acad. Sci. U.S.A.*, 82, 968–972.
22. Moser, H.E. and Dervan, P.B. (1987) *Science*, 238, 645–650.
23. Pailer, M. and Huebsch, W.J. (1966) *Monatsh. Chem.*, 97, 1541–1553.
24. Hobbs, F.W., Jr. (1989) *J. Org. Chem.*, 54, 3420–3422.
25. Meyer, R.B., Jr., Tabone, J.C., Hurst, G.D., Smith, T.M. and Gamper, H. (1989) *J. Am. Chem. Soc.*, 111, 8517–8519.
26. Lin, S.-B., Blake, K.R., Miller, P.S. and Ts'ao, P.O.P. (1989) *Biochemistry*, 28, 1054–1061.
27. Ebright, Y.W., Chen, Y., Pendergrast, P.S. and Ebright, R.H. (1992) *Biochemistry*, 31, 10664–10670.
28. Milligan, J.F., Groebe, D.R., Witherell, G.W. and Uhlenbeck, O.C. (1987) *Nucleic Acids Res.*, 15, 8783–8798.
29. Sambrook, J., Fritsch, E.F. and Maniatis, T. (1989) *Molecular Cloning: A Laboratory Manual 2nd Ed.*, Cold Spring Harbor Laboratory, Cold Spring Harbor.
30. Hakimelahi, G.H., Proba, Z.A. and Ogilvie, K.K. (1982) *Can. J. Chem.*, 60, 1106–1113.
31. Wu, T., Ogilvie, K.K. and Pon, R.T. (1989) *Nucleic Acids Res.*, 17, 3501–3517.
32. Gait, M.J. (1984) *Oligonucleotide Synthesis: A Practical Approach*, IRL Press, Washington DC.
33. Sekharudu, C.Y., Yathindra, N. and Sundaralingam, M. (1993) *J. Biomol. Struct. Dyn.*, 11, 225–244.
34. Iverson, B.L. and Dervan, P.B. (1987) *Nucleic Acids Res.*, 15, 7823–7830.
35. Donis-Keller, H. (1980) *Nucleic Acids Res.*, 8, 3133–3142.
36. Maxam, A.M. and Gilbert, W. (1980) *Methods Enzymol.*, 65, 499–560.